Eur. Phys. J. D (2020) 74: 34
https://doi.org/10.1140/epjd/e2020-100483-7

THE EUROPEAN PHYSICAL JOURNAL D

Regular Article

Positron scattering by the Ar_2 and Xe_2 dimers*

Eliton Popovicz Seidel[a] and Felipe Arretche

Departamento de Física, Universidade Federal de Santa Catarina, 88040-900 Florianópolis, SC, Brazil

Received 30 September 2019 / Received in Final form 14 December 2019
Published online 20 February 2020

Abstract. Positron scattering by Ar_2 and Xe_2 dimers are studied for low incident energies. The Zero Range Potential approximation is used and the dimer is modeled as two independent atoms under an internuclear distance constraint. The scattering calculations are performed within the fixed nuclei and the rigid rotor formulations. For the fixed nuclei approximation, analytical expressions are obtained for the positron-dimer scattering length and for the elastic cross section. In the rigid rotor treatment, an analytical expression is obtained for the rotational excitation cross sections. The main results obtained in this investigation are that the short-range interaction between the positron and the molecular dimer is the dominant mechanism for rotational excitation in this energy range. Such effect is explained by the small values of the quadrupole moments of the Ar_2 and Xe_2 dimers.

1 Introduction

The rare-gas dimers are systems formed by two rare-gas atoms weakly bounded by means of the van der Waals interactions [1]. For this reason, the rare-gas dimers have been extensively studied in order to establish potentials that properly describe their molecular properties [2,3], and such task has shown to be a difficult one. For He_2, for instance, Cybulski and Toczylowski [4] reported an ab initio potential that is not even deep enough to support a vibrational bound state, while it does exist for the potential calculated by Jenzen and Aziz [5].

In the scattering field, there are few works that used the rare-gas dimer as targets. Allan [6], for example, measured the electron impact spectra of Xe_2 and Xe_n ($n = 3, 4$), sweeping the 8.0–8.9 energy-loss range, founding that Feshbach resonances associated to the $Xe\,^3P_2$ and $^3P_1$ atomic lines are practically absent for this dimer. Blanco and Garcia [7] computed electron-Ar_2 elastic and inelastic scattering cross sections between 1 and 500 eV using the screening corrected additivity rule combined with the independent atom representation. Lately, Goswami et. al. [8] calculated, employing a spherical complex optical potential formalism, the total inelastic cross-sections for electron-rare-gas dimers. Applying the Zero Range Potential (ZRP) approximation to study positron scattering by Kr_2, Gribakin [9] demonstrated that positron annihilation with molecules can be strongly enhanced due to Feshbach vibrational resonances. Inspired by this article, Seidel and Arretche [10] studied the rovibrational excitation cross sections of electron scattering by rare-gas dimers, also using the ZRP approximation.

The ZRP approximation is based in the fact that, for small energies, the de Broglie wavelength of the incident particle is much larger than the potential extension, in such a way that the potential may be considered to have a zero range [11,12]. Such successful methodology has been applied several times to treat electron-molecule scattering problems. Drukarev and Yurova used it combined with the adiabatic approximation to calculate rotational and vibrational cross sections for electron-H_2, Li_2, Na_2, and K_2 impact [13]. In a similar way, Ostrovsky and Ustimov obtained the exact solution of the particle-rigid-rotor scattering problem [14]. Later, Gribakin and Lee used the ZRP to explore positron binding to polyatomics and examined the dependence of the binding energy on the size of the molecule for alkanes [15]. Finally, Leble and Yalunin applied the ZRP to calculate the electronic and vibrational excitation cross sections of H_2 by electron impact [16,17].

In this article we study the positron scattering by Ar_2 and Xe_2 dimers employing the ZRP approximation in the same spirit of the investigation performed by Seidel and Arretche for electrons [10]. The application of the ZRP method to van der Waals homonuclear rare-gas dimers is very convenient, once that each rare-gas atom in the dimer causes only a small perturbation in the second one. Due to that, the dimer is modeled as two individual atoms under an internuclear equilibrium distance R_0 constraint. This way of modeling the dimer also allows us to estimate the reach of the short-range potential R_a. Assuming that, as suggested by Franz et al. [18], the matching point between the short-range potential with the long-range asymptotic potential is

* Contribution to the Topical Issue: "Low-Energy Positron and Positronium Physics and Electron-Molecule Collisions and Swarms (POSMOL 2019)", edited by Michael Brunger, David Cassidy, Saša Dujko, Dragana Marić, Joan Marler, James Sullivan, Juraj Fedor.

[a] e-mail: e.p.seidel@posgrad.ufsc.br

close to the Van der Waals radii R_w of the atom, we have $R_a = R_0/2 + R_w$. Considering the internuclear distance of order $R_0 \approx 8a_0$ (the largest value of R_0, corresponding to Xe_2) and $R_w \approx 4a_0$ for the Xe atom [19], we obtain $R_a \approx 8a_0$. As the ZRP approximation is reasonable for very small incident momentum particles, where the condition $kR_a \ll 1$ is respected, we apply such methodology to incident positron energies up to ≈100 meV.

The main goal of this work is to compare the elastic and rotational cross sections obtained in the ZRP approximation with similar models present in literature. In special, the elastic cross section is compared to the theory developed by Fabrikant [20], where the Effective Range Theory (ERT) was applied to study electron scattering by non-polar molecules. The rotational cross sections are compared to the Gerjuoy-Stein (GS) [21] and Dalgarno-Moffett (DM) [22] theories. The GS model applies the Born approximation assuming that the rotational excitation are induced by the long-range interaction between the incident particles with the quadrupole moment of the diatomic molecule. The DM model uses the same approach as the GS model, but also considering the long-range polarization potential.

This paper is organized as follows: Section 2 presents the ZRP theory used in this work. Section 3 presents the atomic and molecular parameters used in the calculation. Section 4 shows the results and the discussion. Finally, the conclusions are reported in Section 5. Atomic units are used throughout the paper.

2 Theory

In the ZRP approximation, the boundary condition for a homonuclear dimer is written as [10]

$$\frac{1}{r\psi(\boldsymbol{r})}\frac{d[r\psi(\boldsymbol{r})]}{dr}\bigg|_{\boldsymbol{r}\to\boldsymbol{R_j}} = -\kappa(k_\nu), \tag{1}$$

where $\boldsymbol{R}_j$ locates the jth nucleus ($j = 1, 2$) and k_ν is the final positron momentum. The $\kappa(k_\nu)$ for the ZRP with Polarization (ZRPP) model is given by:

$$\kappa(k_\nu) = \frac{1}{A} - \frac{\pi\alpha_0}{3A^2}k_\nu - \frac{4\alpha_0}{3A}k_\nu^2\ln(k_\nu), \tag{2}$$

where A is the positron-atom scattering length and α_0 is the dipolar polarizability of the atom. Such expression must depend on the final positron momentum in order to numerically respect the principle of detailed balance (see Sect. IIB4 of Seidel and Arretche [10]). For the ZRP model, i.e., without polarization effects, the $\kappa(k_\nu)$ becomes a simple parameter obtained setting $\alpha_0 = 0$ in (2).

Once that in the ZRP method the asymptotic behavior of the wavefunction becomes the wavefunction itself, we have that:

$$\begin{aligned}\psi(\boldsymbol{r}) = {} & e^{i\boldsymbol{k}_{\nu_i}\cdot\boldsymbol{r}}\Psi_{\nu_i}(\boldsymbol{R}) \\ & + \sum_{\nu'} A_{\nu'}\frac{e^{ik_{\nu'}|\boldsymbol{r}-\boldsymbol{R_1}|}}{|\boldsymbol{r}-\boldsymbol{R_1}|}\Psi_{\nu'}(\boldsymbol{R}) \\ & + \sum_{\nu'} B_{\nu'}\frac{e^{ik_{\nu'}|\boldsymbol{r}-\boldsymbol{R_2}|}}{|\boldsymbol{r}-\boldsymbol{R_2}|}\Psi_{\nu'}(\boldsymbol{R}),\end{aligned} \tag{3}$$

where $\Psi_{\nu'}(\boldsymbol{R})$ is the molecular wavefunction. The label ν' denotes the quantum state configuration of the dimer, while $\boldsymbol{R}$ is the relative internuclear distance ($\boldsymbol{R} = \boldsymbol{R_2} - \boldsymbol{R_1}$). The first term on the right hand side (RHS) of (3) represents an electron with incident momentum $\boldsymbol{k}_{\nu_i}$, which is fixed in the $\hat{z}$ direction, plus a molecule in the initial state $\Psi_{\nu_i}(\boldsymbol{R})$. The sums in the RHS are scattering events which leave the molecule in the ν'-th final state. The energy conservation implies:

$$E_{\nu_i} + \frac{k_{\nu_i}^2}{2} = E_\nu + \frac{k_\nu^2}{2}, \tag{4}$$

where $E_{\nu_i,\nu}$ are the eigenenergies of the initial and final state of the dimer respectively.

Using the wavefunction (3) and the boundary condition (1) we find a system of linear equations for the coefficients $A_\nu^{\nu_i}$ and $B_\nu^{\nu_i}$:

$$\begin{aligned}A_\nu^{\nu_i}(\kappa(k_\nu) + ik_\nu) + \sum_{\nu'} B_{\nu'}^{\nu_i}\left\langle \nu\left|\frac{e^{ik_{\nu'}R}}{R}\right|\nu'\right\rangle \\ = -\langle\nu|e^{i\boldsymbol{k}_{\nu_i}\cdot\boldsymbol{R}/2}|\nu_i\rangle\,,\end{aligned} \tag{5}$$

$$\begin{aligned}B_\nu^{\nu_i}(\kappa(k_\nu) + ik_\nu) + \sum_{\nu'} A_{\nu'}^{\nu_i}\left\langle \nu\left|\frac{e^{ik_{\nu'}R}}{R}\right|\nu'\right\rangle \\ = -\langle\nu|e^{-i\boldsymbol{k}_{\nu_i}\cdot\boldsymbol{R}/2}|\nu_i\rangle\,,\end{aligned} \tag{6}$$

where the matrix elements are:

$$\left\langle \nu\left|\frac{e^{ik_{\nu'}R}}{R}\right|\nu'\right\rangle = \int \Psi_\nu^*(\boldsymbol{R})\frac{e^{ik_\nu R}}{R}\Psi_{\nu'}(\boldsymbol{R})R^2dRd\hat{R}, \tag{7}$$

$$\langle\nu|e^{i\boldsymbol{k}_{\nu_i}\cdot\boldsymbol{R}/2}|\nu_i\rangle = \int \Psi_\nu^*(\boldsymbol{R})e^{i\boldsymbol{k}_{\nu_i}\cdot\boldsymbol{R}/2}\Psi_{\nu_i}(\boldsymbol{R})R^2dRd\hat{R}. \tag{8}$$

The solutions of the matrix elements above depend on how the dimer is described by the molecular wavefunction $\Psi_\nu(\boldsymbol{R})$. In this work, we consider two levels of molecular approximation: the fixed nuclei approximation (FNA) and the rigid rotor approximation (RRA).

Taking the limit $r \to \infty$ in the wavefunction (3), for small energies, the scattering amplitude is obtained

$$f \approx A_\nu^{\nu_i} + B_\nu^{\nu_i}, \tag{9}$$

and the $\nu_i \to \nu$ transition cross section is, therefore:

$$\sigma_{\nu_i\to\nu} = \frac{k_\nu}{k_{\nu_i}}\int |f|^2 d\hat{k}' \approx 4\pi\frac{k_\nu}{k_{\nu_i}}|A_\nu^{\nu_i} + B_\nu^{\nu_i}|^2. \tag{10}$$

2.1 The fixed nuclei approximation

The FNA is the simpler way to describe the dimer. In this approximation, the dimer keeps its original geometrical configuration. This raw treatment greatly simplifies the calculation and it allows us to find an analytical expression for the elastic cross section.

The effective molecular wavefunction product that implies the FNA in the matrix elements (7) and (8) is

$$\Psi_{\nu'}(\boldsymbol{R})\Psi_{\nu_i}^*(\boldsymbol{R}) = \frac{\delta(R-R_0)}{R^2}\delta(\hat{R})\delta_{\nu'\nu_i}, \tag{11}$$

where $\delta(x)$ is the Dirac delta function and $\delta_{\alpha\beta}$ is the Kronecker's delta. The Dirac delta functions in (11) accounts for the fact that in the fixed nuclei approximation, the target does not vibrate nor rotate. Therefore, the molecule remains in its internuclear equilibrium geometry R_0 and in its original space orientation $\hat{R}$. The Kronecker's delta translates the physical scenario where any excitation associated to the nuclear degrees of freedom is fully disregarded. From energy conservation $k_{\nu'} = k_{\nu_i}$.

Solving the system of linear equations the cross section, obtained making use of (10), is

$$\sigma^{\text{elas}}(k_{\nu_i}) \approx \frac{16\pi}{(3-\kappa(k_{\nu_i})R_0)k_{\nu_i}^2 + (\kappa(k_{\nu_i})+1/R_0)^2}. \quad (12)$$

The positron-dimer scattering length A_m is obtained taking the negative value of the scattering amplitude (9) in the limit of $k_{\nu_i} \to 0$:

$$A_m = \frac{2R_0}{\frac{R_0}{A}+1}. \quad (13)$$

Knowing that the isotropic polarizability of the dimer $\alpha_0^{(m)}$ is $\approx 2\alpha_0$ [23], we expand the elastic cross section (12) up to order $\ln(k_{\nu_i})k_{\nu_i}^2$ and write it in terms of the molecular parameters:

$$\sigma^{\text{elas}}(k_{\nu_i}) \approx 4\pi A_m^2 \left(1 + \frac{2\pi\alpha_0^{(m)}}{3A_m}\left[1 + \frac{A_m}{R_0}\left(\frac{A_m}{4R_0} - 1\right)\right]k_{\nu_i} + \frac{4\alpha_0^{(m)}\ln k_{\nu_i}}{3}\left(1 - \frac{A_m}{2R_0}\right)k_{\nu_i}^2\right). \quad (14)$$

An interesting result is obtained considering $|A_m|/R_0 \ll 1$ in the expression above. In such case, from (13) we have that $A_m \approx 2A$, what leads to $\sigma^{\text{elas}} \approx 4\,\sigma_{\text{atom}}^{\text{elas}}$, where $\sigma_{\text{atom}}^{\text{elas}}$ is the positron-atom cross section expansion up to order $\ln(k_{\nu_i})k_{\nu_i}^2$ [24]:

$$\sigma_{\text{atom}}^{\text{elas}}(k_{\nu_i}) \approx 4\pi A^2\left(1 + \frac{2\pi\alpha_0}{3A}k_{\nu_i} + \frac{8\alpha_0\ln k_{\nu_i}}{3}k_{\nu_i}^2\right). \quad (15)$$

As the elastic cross section is proportional to the square of the molecular scattering length, we find the counter-intuitive result that $\sigma_m \approx 4\sigma_{\text{at}}$ and not $\sigma_m \approx 2\sigma_{\text{at}}$ as could be thought by naive geometrical reasons.

2.1.1 Effective Range Theory for molecules

It is also interesting to compare the expression (14) to the analytical results obtained within the Effective Range Theory (ERT) for molecules, developed by Fabrikant [20]. The elastic cross section for a molecule calculated in this approximation is:

$$\sigma_{\text{ert}}^{\text{elas}} \approx 4\pi A_m^2\left(1 + \frac{2\pi\alpha_0^{(m)}}{3A_m}k_{\nu_i} + \frac{8\alpha_0^{(m)}\ln k_{\nu_i}}{3}k_{\nu_i}^2\right). \quad (16)$$

In the original work of Fabrikant [20], the expression above depends on the quadrupole moment Q and on the product of the quadrupole moment with the anisotropic polarizability $\alpha_2^{(m)}$ of the molecule. However, as the rare-gas dimers have small values of Q (see Sect. 3), these terms do not significantly contribute to the elastic cross section and have been neglected in (16). One may notice comparing (14) with (16) that the linear term of (14) becomes equal to the ERT results (16) if $|A_m|/R_0 \ll 1$. The term proportional to $\ln(k_{\nu_i})k_{\nu_i}^2$, nevertheless, differs by a factor of 2 even in this situation. Therefore, the expressions (14) and (16) shall provide different results once that $|A_m|/R_0$ is not a small number for the rare-gas dimers studied in this work.

2.2 The rigid rotor approximation

In the RRA, the rotational degrees of freedom of the dimer are accounted, and rotational transitions may happen induced by the collision process with the positron. In general, the coupling of the rotational states with the vibrational ones can affect the rotational cross section. However, in reference [10] it is shown that, in the ZRP model, the effects of the vibrational states is only appreciable in the rotational cross section if the vibrational constant is close to the rotational constant of the dimer, which is not the case for Xe_2 and Ar_2. Therefore, the RRA provides results precise as a rovibrational approximation.

As the rare-gas dimers are linear molecules, the rotational eigenfunctions are simple spherical harmonics $Y_{JM}(\hat{R})$, where J and M are the rotational quantum numbers [25]. Therefore, the effective molecular wavefunction product that translates the RRA into the matrix elements (7) and (8) is

$$\Psi_{JM}(\boldsymbol{R})\Psi^*_{J'M'}(\boldsymbol{R}) = \frac{\delta(R-R_0)}{R^2}Y_{JM}(\hat{R})Y^*_{J'M'}(\hat{R}). \quad (17)$$

The rotational energy of the dimer is:

$$E_J = BJ(J+1), \quad (18)$$

where B is the rotational constant. Solving the system of linear equations and using (10), the cross section, obtained taking the average on the initial rotational projections M_i and summing over the rotational projections M, is:

$$\sigma_{J_i\to J}(k_{J_i}) = \sigma_{0\to J}(k_{J_i})\sum_{L=J-J_i}^{J+J_i}\left(\frac{k_{J_i}R}{2}\right)^{2(L-J)} \times \left[\frac{(2J+1)!!\,\langle J0J_i0|L0\rangle}{(2L+1)!!}\right]^2 \quad (19)$$

where $\langle J_1M_1J_2M_2|JM\rangle$ are the Clebsh-Gordan coefficients and, for small momenta, the $0 \to J$ transition cross

section is:

$$\sigma_{0\to J}(k_0) = \frac{k_J}{k_0}\left[\frac{(k_0R_0)^J}{2^J(2J+1)!!}\right]^2 \times \frac{16\pi(2J+1)}{(3-\kappa(k_J)R_0)k_J^2+(\kappa(k_J)+1/R_0)^2}. \quad (20)$$

The rotational cross section may also be obtained using the adiabatic approximation (ADA) [13,14], where the transition amplitude is calculated using the relation

$$f^{(\mathrm{ADA})}_{J_iM_i\to JM} = \int Y^*_{JM}(\hat{R}) f^{(\mathrm{FNA})} Y_{J_iM_i}(\hat{R}) d\hat{R}, \quad (21)$$

where $f^{(\mathrm{FNA})}$ is the scattering amplitude calculated in the fixed nuclei approximation. The $0 \to J$ transition cross section is, therefore:

$$\sigma^{\mathrm{ADA}}_{0\to J}(k_0) = 16\pi\frac{k_J}{k_0}(2J+1)\sum_{l=0}^{\infty}\sum_{l'=|l-J|}^{l+J}(2l'+1) \times\left|\frac{j_l(k_0R_0/2)j_{l'}(k_JR_0/2)}{\kappa(k_J)+ik_J+(-1)^l\frac{e^{ik_JR_0}}{R_0}.}\right|^2\langle J0l'0|l0\rangle^2. \quad (22)$$

Comparing (20) with (22) we find that the ADA result presents larger magnitude than the one obtained by calculating the coefficients $A^{J_iM_i}_{\mathrm{JM}}$ and $B^{J_iM_i}_{\mathrm{JM}}$. This is due to the fact that these coefficients are considered to be independent of $\boldsymbol{r}$ in the wavefunction (3), what leads to an isotropic scattering in the RRA. The $0 \to J$ transition cross section (20), therefore, needs a correction in order to account for the missing anisotropic partial waves. In the Appendix A, considering the low energy regime, we show that:

$$\sigma^{\mathrm{ADA}}_{0\to J}(k_0) \approx \sigma_{0\to J}(k_0)\; g_{0J}, \quad (23)$$

where $\sigma_{0\to J}(k_0)$ is given by (20), and g_{0J} is the correction factor:

$$g_{0J} = \sum_{l=0}^{J}\left[\frac{\sqrt{2(J-l)+1}(2J+1)!!}{(2l+1)!!(2[J-l]+1)!!}\right]^2 \times\left[\frac{\langle J0(J-l)0|l0\rangle\,(R_0+A)}{(R_0+(-1)^lA)}\right]^2. \quad (24)$$

The correction factor g_{0J} lead us to conclude that applying the ZRP as it was done in this section only accounts for the $l = 0$ partial wave (note that the contribution of $l = 0$ to g_{0J} is equal to one). However, due to the spherical Bessel properties exploited in Appendix A, it is shown that the contribution of the missing partial waves ($l = 1, \ldots, J$) to the rotational cross section has, basically, the same energy dependence as the $l = 0$ one. Therefore, the correction factor acts to adjust the rotational cross section magnitude in order to match it with the one that had all partial waves considered.

2.2.1 Gerjuoy-Stein and Dalgarno-Moffett models

One of the most successful models for describing rotational transitions of homonuclear diatomic molecules is the one formulated by Gerjuoy and Stein (GS) [21]. It works with the hypothesis that the long-range positron interaction with the quadrupole moment Q of the homonuclear molecules is the dominant mechanism for rotational excitation. The GS rotational cross section for a transition $J \to J+2$ is given by

$$\sigma^{\mathrm{GS}}_{J\to J+2} = \frac{k_{J+2}}{k_J}\frac{8\pi}{15}Q^2\frac{(J+2)(J+1)}{(2J+3)(2J+1)}. \quad (25)$$

For the Ar_2 and Xe_2 dimers studied in this work, due to the small value of the rotational constant B see Section 3, the GS rotational cross section becomes flat for energies above $\approx$1 meV, where $k_J \approx k_{J+2}$. The magnitude of the cross section is determined by the square of the quadrupole moment of the dimer. As these values are small, the GS rotational cross section presents a small magnitude as well.

Later, a generalization of the GS model was proposed by Dalgarno and Moffet (DM) [22], where the polarization effects of the homonuclear molecule was included in the calculation. Due to symmetry arguments, only the anisotropic polarization $\alpha_2^{(m)}$ contributes to the rotational excitation in the collision process. The DM rotational cross section for positron-homonuclear molecule is

$$\sigma^{\mathrm{DM}}_{J\to J+2} = \sigma^{\mathrm{GS}}_{J\to J+2}\left(1-\frac{\pi\alpha_2^{(m)}}{4Qk_J}\left[k_J^2-\frac{\Delta k^2}{4}\right] +\frac{9\pi^2}{512}\left(\frac{\alpha_2^{(m)}}{Q}\right)^2\left[k_J^2-\frac{\Delta k^2}{2}\right]\right), \quad (26)$$

where

$$\Delta k^2 = k_J^2 - k_{J+2}^2 = 4(2J+3)B. \quad (27)$$

Once Q is negative for the Ar_2 and Xe_2 dimers, the polarization contribution of the DM model for the rotational cross section (26) enhances the magnitude of the rotational cross section in respect to the GS model.

3 Parameters of the model

There are two atomic parameters required in the ZRPP model: the atomic dipolar polarizability α_0 and the positron-atom scattering length A. The values of these parameters used in this work are $\alpha = 11.1$ [26] and $A = -4.41$ [27] for Ar, while, for Xe, $\alpha = 27.3$ [26] and $A = -84.5$ [27].

Regarding the dimer, the parameters needed for the ZRP and ZRPP calculations are the reduced dimer mass μ and the equilibrium internuclear distance R_0. The rotational constant B is also required in the RRA, but it can be calculated using the reduced mass and equilibrium configuration through the relation $B = 1/2\mu R_0^2$. For the ERT model, the molecular isotropic polarizability $\alpha_0^{(m)}$ is required. This parameter, for Ar_2 and Xe_2, is

Table 1. Molecular parameters of Ar_2 and Xe_2 in atomic units: reduced mass μ, equilibrium position R_0, rotational constant B, quadrupole moment Q, molecular isotropic polarizability $\alpha_0^{(m)}$ and molecular anisotropic polarizability $\alpha_2^{(m)}$.

	$\mu/10^3$	R_0	$B/10^{-7}$	$Q/10^{-2}$	$\alpha_0^{(m)}$	$\alpha_2^{(m)}$
Ar_2	33.0	7.10[a]	3.00	−1.86[c]	22.2	2.05[e]
Xe_2	99.1	8.24[b]	0.731	−3.92[d]	54.6	8.52[f]

[a]Reference [28]; [b]reference [29]; [c]reference [30]; [d]reference [31]; [e]reference [32]; [f]reference [33].

obtained using the relation $\alpha_0^{(m)} \approx 2\alpha_0$, where α_0 is the dipolar polarizability of the respective rare-gas atom. The GS rotational cross section depends on the quadrupole moment of the target Q, while the DM model depends on Q and also on the molecular anisotropic polarizability $\alpha_2^{(m)}$. All the required parameters are presented in Table 1 for the Ar_2 and Xe_2 dimers.

4 Results and discussion

In this section, the ZRP and ZRPP elastic cross sections for Ar_2 and Xe_2 calculated in the FNA are compared to the ERT results of Fabrikant [20], as discussed in Section 2.1.1. On the other hand, the ZRP and ZRPP rotational cross sections for both dimers, calculated in the RRA, are compared with the Gerjuoy-Stein (GS) and Dalgarno-Moffett (DM) theories, as described in Section 2.2.1.

4.1 Positron-Ar_2

For comparing the elastic cross section obtained with the ZRP approximation with the ERT one, we make use of the expressions (14) and (16). The ZRPP result for small momentum is

$$\sigma^{\text{elas}}(k) \approx 6810[1 - 13.94k + 78.14\ln(k)k^2], \tag{28}$$

meanwhile, the ERT result reads

$$\sigma^{\text{elas}}_{\text{ERT}}(k) \approx 6810[1 - 2.00k + 59.30\ln(k)k^2]. \tag{29}$$

These expressions show that the linear and $\ln(k)k^2$ components of the ZRPP elastic cross section are, respectively, ≈7.0 and ≈1.3 times higher than the ERT one. In practice, this indicates that the introduction of the polarization in the ZRP model leads to an elastic cross section that varies with k much faster than the ERT result. In both expressions the contribution from the terms that depend on the dimer polarization are negative, once that $\ln(k) < 0$ for $k < 1$. As consequence, the polarization effects make the magnitude of the elastic cross section to decrease in respect to the result where the target is static.

Figure 1 shows the results for the elastic cross section for positron-Ar_2. The ZRP and ZRPP results are obtained with expression (12) rather than (28). The reason for this is simply because expression (12) is valid for energies higher than (28). The ZRPP line (solid line with squares) has lower magnitude when compared to the ZRP one (solid line with circles). This is expected, once that, as discussed above, the terms that come from the inclusion of polarization effects have negative contribution in the elastic cross section.

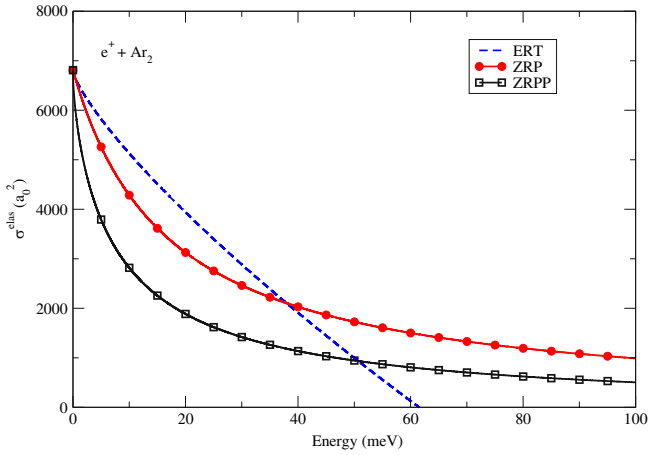

Fig. 1. Elastic cross section for positron-Ar_2. Solid line with circles: ZRP result obtained setting $\alpha_0 = 0$ in expression (12); solid line with squares: ZRPP result, obtained using expression (12); dashed line: ERT result, obtained using expression (16). All the parameters used are present in Section 3.

The elastic cross section provided by the ERT (dashed line) is also presented in Figure 1. The ZRPP elastic cross section is, in fact, lower in magnitude than the ERT for energies up to 50 meV. One may easily explain this result by looking into expressions (28) and (29). It is interesting to observe, nonetheless, that even the ZRP result has lower magnitude than the ERT one. In order to understand this result, we set $\alpha_0 = 0$ in (12) and expand it for small k:

$$\sigma^{\text{elas}}_{\text{ZRP}}(k) \approx 4\pi A_m^2 \left(1 + \left[\frac{R_0}{2A_m} - 1\right] A_m^2 k^2\right), \tag{30}$$

which, using the Ar_2 parameters, results in:

$$\sigma^{\text{elas}}_{\text{ZRP}}(k) \approx 6810\left(1 - 624.07k^2\right). \tag{31}$$

The expression above reveals that the quadratic contribution for the elastic cross section is significant even for very low energies due to the value that multiply k^2. It suggests that the ERT result reaches its limitation for a very small value of energy, once that terms of order k^2 are not present on the elastic cross section.

Figure 2 shows the rotational cross section for a transition $0 \to 2$ calculated in the RRA. The effects of the polarization accounted in the ZRPP (solid line with square) affect mainly the magnitude of the rotational cross section when compared to the pure ZRP one (solid line with circles). In fact, the magnitude of the ZRP result is ≈1.9 times higher than the ZRPP, while the dependence on the energy is very similar in both approaches. As discussed in 2.2, in order to account for the missing partial waves the

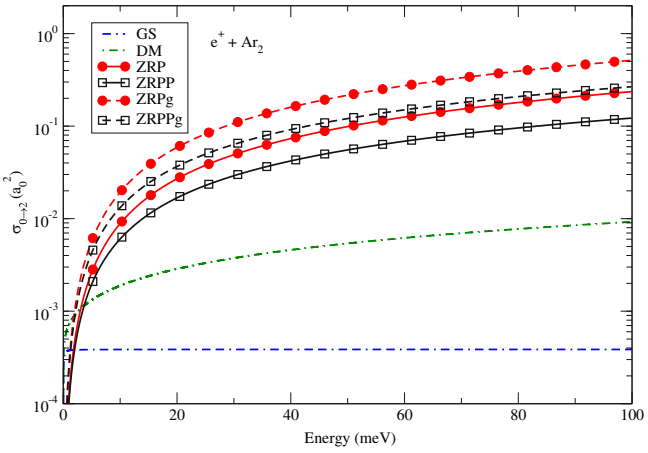

Fig. 2. $0 \rightarrow 2$ rotational cross section for positron-Ar_2. Solid line with circles: ZRP result obtained setting $\alpha_0 = 0$ in (20); solid line with squares: ZRPP results obtained with expression (20); dashed line with circles: ZRP rotational cross section multiplied by the correction factor (24); dashed line with squares: ZRPP rotational cross section multiplied by the correction factor (24); dash-dash-dotted line: GS rotational cross section, obtained through (25); dash-dotted line: DM rotational cross section, obtained through (26). All the molecular parameters used in the calculation are presented in Section 3.

ZRP/ZRPP results must be multiplied by a factor g_{0J}. For $J = 2$, the correction factor takes a simple form:

$$g_{02} = 2 + \frac{10}{3}\left(\frac{R_0 + A}{R_0 - A}\right)^2, \tag{32}$$

which results in ≈2.18 for positron-Ar_2. In Figure 2, the rotational cross section multiplied by the correction factor is denominated ZRPg (dashed line with circles) and ZRPPg (dashed line with squares). The GS (dash-dash-dotted line) and the DM (dash-dotted) rotational cross sections are also shown. The GS rotational cross section becomes a constant, with magnitude of $\approx 1.10 \times Q^2 = 3.8 \times 10^{-4}$, very early in the energy, due to the small value of the rotational constant $B \approx 8.0 \times 10^{-3}$ meV. The effect of the asymptotic polarization potential in the DM model makes the rotational cross section to increase with the energy, becoming at least one order of magnitude higher than the GS result. Even this way, for energies higher than ≈1 meV, all the results obtained using the ZRP approximation are much higher in magnitude than the GS and DM ones. The reason for that comes from the small value of the quadrupole moment Q. This leads us to conclude that the short-range interactions is the dominant mechanism for rotational excitation positron-Ar_2 collision.

4.2 Positron-Xe_2

The study of positron-Xe_2 is interesting due to the large value of the positron-Xe scattering length: $A = -84.5$. In this case, the positron-Xe_2 scattering length, calculated through (13), is $A_m \approx 18.26$. The first thing that deserves attention is the fact that the composition of two atoms with negative scattering length A forms a dimer with a positive scattering length A_m. Secondly, the elastic cross section of positron-Xe is $(A/A_m)^2 \approx 21$ times higher than the respective cross section for positron-Xe_2 in the low energy limit.

For the positron-Xe_2 ZRPP elastic cross section expansion (14) is

$$\sigma^{\text{elas}}(k) \approx 4190[1 + 0.076k - 8.00\ln(k)k^2], \tag{33}$$

and the ERT one (16) is

$$\sigma^{\text{elas}}_{\text{ert}}(k) \approx 4190[1 + 6.26k + 145.60\ln(k)k^2]. \tag{34}$$

The linear term of the ERT result is $\approx 10^2$ higher than the ZRPP one. Regarding the $\ln(k)k^2$ term, the difference is also present in the algebraic sign. In the ZRPP elastic cross section, the polarization contribution is positive, while in the ERT expression the $\ln(k)k^2$ contribution is negative.

Figure 3 brings the elastic cross section obtained within the ZRP and ZRPP models calculated through (12) compared with the ERT result. The difference between the ZRP (solid line with circles) and the ZRPP (solid line with squares) is minimum. This may be understood observing, in expression (33), that the corrections due to the polarizability are small.

Once that the Xe_2 isotropic polarizability value is larger than the Ar_2 one (see Tab. 1), its small contribution to the elastic cross section is physically counter-intuitive. The first step to understand this result is to note that the polarization effect in the cross section for positron-Xe is also small. This is a consequence of the very large value of positron-Xe scattering length A, causing a small ratio α_0/A in the relation (15). In a given sense, one can interpret this ratio as a "competition" between the short-range potential, represented by the scattering length A, and the long-range polarization potential, represented by the isotropic polarizability α_0. Therefore, the small ratio of α_0/A suggests that the short-range potential is the dominant mechanism for positron-Xe scattering (this is not the case for electron-Xe, for example, as it may be seen in [10]). For the positron-Xe_2, this competition between the short-range and the long-range potentials effects is represented taking the coefficient that multiplies the linear term of the expression (14), which may be written as:

$$\frac{\alpha_0^{(m)}}{A_m}\left[1 + \frac{A_m}{R_0}\left(\frac{A_m}{4R_0} - 1\right)\right] \propto \frac{\alpha_0^{(m)} A_m}{A^2}. \tag{35}$$

The right hand side of the relation above is still small due to the large value of A. Thus, the polarization contribution to the elastic cross section for positron-Xe_2 is small, suggesting that the short-range potential is also the dominant mechanism for this case, similarly to the positron-Xe case. This is not a surprise since the dimer was modeled as two independent Xe atoms.

For the ERT result in Figure 3, the term proportional to $\ln(k)k^2$ dominates the linear one and the cross section decreases with the energy (dashed line). Similarly to the positron-Ar_2 case, the quadratic order of the cross section plays an important role, once that, from expression (30):

$$\sigma^{\text{elas}}_{\text{ZRP}}(k) \approx 4190\left(1 - 258.20k^2\right). \tag{36}$$

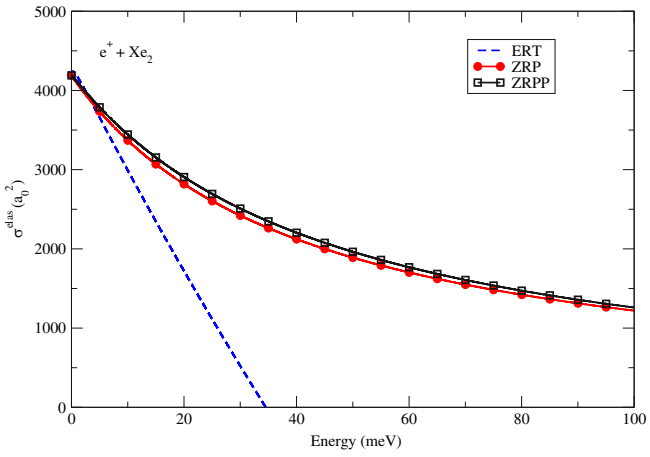

Fig. 3. Same as Figure 1, but for positron-Xe_2.

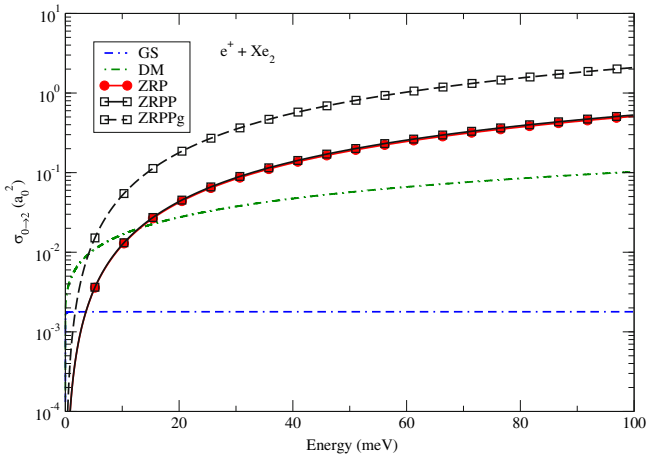

Fig. 4. Same as Figure 2, but for positron-Xe_2.

Figure 4 presents the $0 \rightarrow 2$ rotational cross section for positron-Xe_2. As observed in the elastic cross section (see Fig. 3), the ZRPP result (solid line with squares) is very close to the ZRP one (solid line with circles). For this case, from (32) $g_{02} \approx 4.25$, and the ZRPPg (dashed line with squares) rotational cross section is obtained multiplying the ZRPP result by this factor. Similarly to the positron-Ar_2, the ZRPPg model provides results that are much higher in magnitude than the GS model (dash-dash-dotted line) and the DM (dash-dotted line) for energies above $\approx$2 meV. This strongly suggests that the long-range quadrupole potential plays an important role for rotational excitation only for energies close to the rotational threshold, while the short-range interactions are dominant for higher energies.

5 Conclusions

The ZRP approximation was used to investigate the elastic and rotational cross section in scattering by Ar_2 and Xe_2. The dimer is described as two rare-gas atoms under an internuclear constraint characterized by its molecular parameters. Going beyond the original ZRP approach, the polarization effects have been included in the model [10]. This new prescription is called Zero Range Potential with Polarization (ZRPP).

The fixed nuclei approximation is used in order to obtain analytical expressions for the elastic cross section. It is found that the introduction of the polarization in the ZRP model impacted in the elastic cross section for the positron-Ar_2 when compared to the pure ZRP result. For positron-Xe_2, however, the ZRPP approximation provides results similar to the pure ZRP ones.

The elastic cross sections are compared to the ERT ones, developed by Fabrikant [20]. Once that the Ar_2 and Xe_2 dimers have very small quadrupole moments, the ERT elastic cross section is numerically independent of Q in the energy range studied. It is found that, although the ZRPP elastic cross section presents the same functional form present in the ERT ones, the coefficients are very different, leading to very distinct results. It is also observed that the elastic cross section dependence on terms of quadratic order of the positron momentum, not present in the ERT, play an important role even for energies up to 100 meV for positron-Ar_2 and positron-Xe_2.

Rotational cross sections are obtained in the Rigid Rotor approximation within the ZRP and ZRPP approaches. As discussed in Seidel and Arretche [10], the wavefunction used is approximated in the rigid rotor approximation. As consequence, the rotational cross section presents the correct dependence on the positron momentum, but with lower magnitude when compared with the adiabatic approximation. This leads to the calculation of a correction factor g_{0J} that adjust the rotational cross section magnitude accounting for the missing partial waves of the wavefunction.

The rotational cross sections obtained through the ZRP methodology are, in general, higher in magnitude than the ones obtained using the Gerjuoy-Stein [21] and Dalgarno-Moffet [22] models for energies above $\approx$2 meV. The main reason for it is the small value of the quadrupole moment for both Ar_2 and Xe_2 dimers. This lead us to conclude that, opposed to what is observed in molecules like H_2 and N_2, the short-range interaction between the positron and the molecular dimer is the dominant mechanism for rotational excitation in this energies range. In spite of that, the interaction of the positron with the quadrupole moment dominates for energies below 2 meV.

E. P. Seidel would like to thank the Conselho Nacional de Desenvolvimento Científico de Tecnológico (CNPq) for the financial support. The authors would like to thank the Programa de Pós-Graduação em Física of Universidade Federal de Santa Catarina (UFSC) for computational and technical support.

Author contribution statement

EP Seidel leaded the project, developing the theoretical and computational tools. F Arretche advised the project contributing to discussions, manuscript revision and suggestions for further investigations.

Appendix A: Rotational correction factor

In this Appendix we present the calculation of the correction factor g_{0J} (24). To calculate such factor, we start analyzing the rotational cross section obtained in the ADA (22). The ADA is valid under the condition that $E \gg B$, where E is the positron energy and B is the rotational constant of the dimer. Due to that, and also noting that the B values of the rare-gas dimers are small, $k_0 \approx k_J$ is a reasonable approximation that may be considered in the ADA cross section. Another simplification that can be made in expression (22) comes from the fact that for $x \ll 1$, we have $j_a^2(x) \gg j_b^2(x)$ for $b > a$. Thus, only the lowest order of l' ($l' = |l - J|$ in this case) of (24) plays a considerable role in the total rotational cross section, and the expression is, therefore, simplified to:

$$\sigma_{0\to J}^{\mathrm{ADA}}(k_0) \approx 16\pi \frac{k_J}{k_0}(2J+1)\sum_{l=0}^{\infty}(2|l-J|+1) \times \langle J0(|l-J|)0|l0\rangle^2 \left| \frac{j_l(k_0R_0/2)j_{|l-J|}(k_0R_0/2)}{ik_J + \kappa(k_J) + (-1)^l \frac{e^{ik_0R_0}}{R_0}} \right|^2. \tag{A.1}$$

As the ZRP method is only valid in the low energy regime, we may write the spherical Bessel functions present in (A.1) as its asymptotic behavior for small arguments:

$$j_l^2(x) j_{|l-J|}^2(x) \propto x^{2(l+|l-J|)} \tag{A.2}$$

where $x = k_0R_0/2$. There are two situations that must be analyzed from the relation above:

1. If $l \leq J$, than $l + |l - J| = J$. This implies in the product of the spherical Bessel functions in (A.2) being proportional to x^{2J}, and, therefore, independent of l.
2. If $l > J$, than $l + |l - J| = 2l - J > J$. This lead us to conclude that that partial waves of $l > J$ do not contribute significantly to the rotational cross section in the low energy regime, once that $x^{2J} \gg x^{2l-J}$ for $x \ll 1$.

Considering the argumentation above and using the asymptotic form of the spherical Bessel function, the expression (A.1) is simplified into:

$$\sigma_{0\to J}^{\mathrm{ADA}}(k_0) \approx 16\pi \frac{k_J}{k_0}(2J+1)\left(\frac{k_0R_0}{2}\right)^{2J} \times \sum_{l=0}^{J} \frac{\langle J0(J-l)0|l0\rangle^2}{[(2l+1)!!(2(J-l)+1)!!]^2} \times \frac{(2(J-l)+1)}{[1+(-1)^l(2-\kappa(k_J)R_0)]k_J^2 + \left(\kappa(k_J) + \frac{(-1)^l}{R_0}\right)^2}. \tag{A.3}$$

Comparing the expression above with (20), for $k_0R_0 \ll 1$, we find:

$$\sigma_{0\to J}^{\mathrm{ADA}}(k_0) \approx \sigma_{0\to J}(k_0) \sum_{l=0}^{J} \left[\frac{\sqrt{2(J-l)+1}(2J+1)!!}{(2l+1)!!(2[J-l]+1)!!}\right]^2 \times \left[\frac{\langle J0(J-l)0|l0\rangle\,(R_0+A)}{(R_0+(-1)^lA)}\right]^2, \tag{A.4}$$

which is rewritten as

$$\sigma_{0\to J}^{\mathrm{ADA}}(k_0) \approx \sigma_{0\to J}(k_0) g_{0J}, \tag{A.5}$$

such that the correction factor is:

$$g_{0J} = \sum_{l=0}^{J} \left[\frac{\sqrt{2(J-l)+1}(2J+1)!!}{(2l+1)!!(2[J-l]+1)!!}\right]^2 \times \left[\frac{\langle J0(J-l)0|l0\rangle\,(R_0+A)}{(R_0+(-1)^lA)}\right]^2. \tag{A.6}$$

And finally, we find expression (24).

References

1. Y.-T. Chen, K. Hui, J.-D. Chai, Phys. Chem. Chem. Phys. **18**, 3011 (2016)
2. P. Slavik, R. Kalus, P. Paka, I. Odvrkov, P. Hobza, A. Malijevsk, J. Chem. Phys. **119**, 2102 (2003)
3. K.T. Tang, J.P. Toennies, J. Chem. Phys. **118**, 4976 (2003)
4. S.M. Cybulski, R.R. Toczyowski, J. Chem. Phys. **111**, 10520 (1999)
5. A.R. Janzen, R.A. Aziz, J. Chem. Phys. **107**, 914 (1997)
6. M. Allan, J. Phys. B: At., Mol. Opt. Phys. **26**, L73 (1993)
7. F. Blanco, G. Garca, J. Phys: Conf. Ser. **438**, 012012 (2013)
8. B. Goswami, R. Naghma, B. Antony, Mol. Phys. **111**, 3047 (2013)
9. G. Gribakin, Nucl. Instrum. Methods Phys. Res. B **192**, 26 (2002)
10. E.P. Seidel, F. Arretche, Phys. Rev. A **98**, 052707 (2018)
11. Y.N. Demkov, V.N. Ostrovskii, *Zero-Range Potentials and Their Applications in Atomic Physics* (Springer, Boston, MA, US, 1988)
12. E. Popovicz Seidel, F. Arretche, Am. J. Phys. **87**, 796 (2019)
13. G.F. Drukarev, I.Y. Yurova, J. Phys. B: At., Mol. Opt. Phys. **10**, 3551 (1977)
14. V.N. Ostrovsky, V.I. Ustimov, J. Phys. B: At., Mol. Opt. Phys. **16**, 991 (1983)
15. G. Gribakin, C. Lee, Nucl. Instrum. Methods Phys. Res. B **247**, 31 (2006)
16. S. Leble, S. Yalunin, Phys. Lett. A **306**, 35 (2002)
17. S. Leble, S. Yalunin, Radiat. Phys. Chem. **68**, 181 (2003)
18. J. Franz, K. Fedus, G.P. Karwasz, Eur. Phys. J. D **70**, 155 (2016)
19. J. Vogt, S. Alvarez, Inorg. Chem. **53**, 9260 (2014)
20. I.I. Fabrikant, J. Phys. B: At., Mol. Phys. **17**, 4223 (1984)
21. E. Gerjuoy, S. Stein, Phys. Rev. **97**, 1671 (1955)
22. A. Dalgarno, R. Moffett, Proc. Natl. Acad. Sci. India A **33**, 511 (1963)
23. P.D. Dacre, Mol. Phys. **45**, 1 (1982)
24. T.F. O'Malley, Phys. Rev. **130**, 1020 (1963)
25. W. Demtröder, *Atoms, Molecules and Photons: An Introduction to Atomic, Molecular and Quantum Physics* (Springer, New York, NY, 2010)

26. T.M. Miller, B. Bederson, Atomic and molecular polarizabilities-a review of recent advances, in *Advances in Atomic and Molecular Physics* (Academic Press, 1978), Vol. 13, pp. 1–55
27. D.G. Green, J.A. Ludlow, G.F. Gribakin, Phys. Rev. A **90**, 032712 (2014)
28. T.P. Haley, S.M. Cybulski, J. Chem. Phys. **119**, 5487 (2003)
29. P. Jerabek, O. Smits, E. Pahl, P. Schwerdtfeger, Mol. Phys. **116**, 1 (2018)
30. A.G. Donchev, Phys. Rev. A **76**, 042713 (2007)
31. G. Maroulis, Chem. Phys. Lett. **647**, 114 (2016)
32. G. Maroulis, J. Phys. Chem. A **104**, 4772 (2000)
33. G. Maroulis, A. Haskopoulos, D. Xenides, Chem. Phys. Lett. **396**, 59 (2004)